Selected topics in tau physics from *BABAR*

S.Paramesvaran (on behalf of the *BABAR* Collaboration)
Department of Physics, Royal Holloway, University of London, Egham, Surrey, TW20 0EX, UK

Selected results from τ analyses performed using the *BABAR* detector at the SLAC National Accelerator Laboratory are presented. A precise measurement of the τ mass and the $\tau^+\tau^-$ mass difference is undertaken using the hadronic decay mode $\tau^\pm \to \pi^+\pi^-\pi^\pm\nu_\tau$. In addition an investigation into the strange decay modes $\tau^- \to K^0_S\pi^-\pi^0\nu_\tau$ and $\tau^- \to K^0_S\pi^-\nu_\tau$ is also presented, including a fit to the $\tau^- \to K^0_S\pi^-\nu_\tau$ invariant mass spectrum. Precise values for M(K*(892)) and Γ(K*(892)) are obtained.

1. Introduction

Although the *BABAR* detector [1] was conceived as an experiment to test CP-violation in the B meson system, the cross-section for τ pairs (0.9 nb) is almost as high as that for $b\bar{b}$(1.1 nb). This makes *BABAR* an excellent place to study τ physics. I present preliminary results from studies of tau decays to hadronic final states which provide precise measurements on the τ mass, the $\tau^+\tau^-$ mass difference (Section 2), and information on the branching ratios and mass spectra of the strange hadronic decays $\tau^- \to K^0_S\pi^-\nu_\tau$ and $\tau^- \to K^0_S\pi^-\pi^0\nu_\tau$ (Section 3).

2. Precise measurement of τ mass and $\tau^+\tau^-$ mass difference

A key test of CPT invariance is to measure the difference in mass between a particle and its antiparticle. Using 423 fb^{-1} of data from the *BABAR* detector, a pseudomass endpoint method was used to measure the mass of the τ lepton [2]. The significant advantage in using this method is that it allows the mass of the τ^+ and $\tau-$ to be measured independently, which allows us to test CPT invariance.

The current world average of τ mass is 1776.84± 0.17 MeV/c^2 [3], and the mass difference is $M_{\tau^+} - M_{\tau^-} < 2.8 \times 10^{-4}$ at 90% confidence level.

The pseudomass endpoint method was first used by the ARGUS [4] collaboration, and has since been employed by BELLE [5]. The premise is first to consider reconstructing the mass of the τ from the final state hadronic products ($\tau^- \to h^-\nu_\tau$):

$$M_\tau = \sqrt{M_h^2 + 2(\sqrt{s}/2 - E_h^*)(E_h^* - P_h^*\cos\theta^*)}, \quad (1)$$

where M_h, E_h and P_h are the mass, energy, and magnitude of the three-momentum of the hadronic system h, respectively, θ^* is the angle between the hadronic system and the ν_τ; the * represents quantities in the e^+e^- center-of-mass frame. The relationship $E^*_\tau = \sqrt{s}/2$ is used, where $\sqrt{s}$ is the initial e^+e^- CM energy (10.58 GeV), and E^*_τ is the energy of the τ. In the above representation the angle θ^* is unknown as the neutrino escapes undetected; we therefore define the pseudomass M_p with the condition that $\theta^* = 0$. This simplifies the above equation:

$$M_p = \sqrt{M_h^2 + 2(\sqrt{s}/2 - E_h^*)(E_h^* - P_h^*)}. \quad (2)$$

The distribution of M_p has a sharp kinematic cutoff at $M_p = M_\tau$, although there will be smearing due to initial and final state radiation, and limited detector resolution. The signal mode chosen for this study is $\tau^\pm \to \pi^+\pi^-\pi^\pm\nu_\tau$, due in part to its high branching fraction, $(9.03 \pm 0.06) \times 10^{-2}$ [3], and the ability to obtain high signal purity. The data are then fitted to an empirical function:

$$F(x) = (p_3 + p_4 x)\tan^{-1}\frac{(p_1 - x)}{p_2} + p_5 + p_6 x, \quad (3)$$

where the p_i are the parameters and x is the pseudomass. A relationship between p_1 ,the endpoint parameter, and the pseudomass is required. This is determined from Monte Carlo studies; three different samples are generated with different tau mass values and these are fitted with the function defined above. A straight line is then fitted to the resulting p_1 values, which provides the relation to M_τ. The data are split into two samples according to the total charge of the 3π hadronic final state, and each sample is analyzed independently. The results of these fits are shown in Figure 1. This yields an M_τ of 1776.68 ± 0.12(stat) MeV/c^2. A number of systematic effects are investigated, including potential uncertainties on energy loss measurements for charged particles, and uncertainties in the magnetic field. However, the dominant uncertainty is found to be due to an underestimation of the reconstructed track momenta in the detector model. This contributes 0.39 MeV to a total systematic uncertainty of 0.41 MeV.

3. Strange hadronic tau decays

Strange hadronic tau decays offer a very clean environment for studying the weak current. The branching ratios feed directly into a measurement of V_{us},

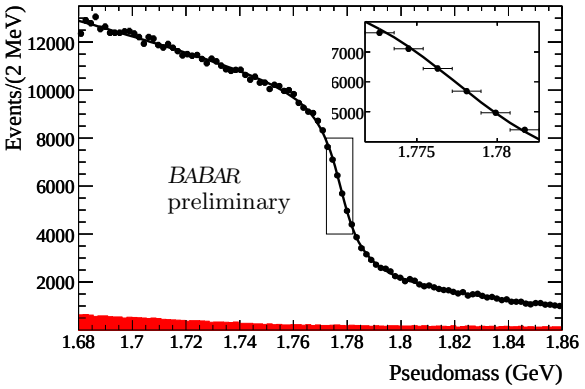

Figure 1: Combined τ^+ and τ^- pseudomass endpoint distribution. The points show the data, the curve is the fit to the data, and the solid area is the background. The inset is an enlargement of the boxed region around the edge position showing the fit quality where p1 is most sensitive.

and fits to the mass spectra can yield resonance parameter values which can further our understanding of the dynamics of these systems. In this section studies are presented of the hadronic mass distributions for the decays $\tau^- \to K^0_S\pi^-\nu_\tau$ and $\tau^- \to K^0_S\pi^-\pi^0\nu_\tau$ (throughout the note, charge conjugate modes are implied). A fit to the invariant mass spectrum from $\tau^- \to K^0_S\pi^-\nu_\tau$ is presented along with precise resonance parameter values of the dominant K*(892)$^-$. Due to this mass spectrum having a peaking background from $\tau^- \to K^0_S\pi^-\pi^0\nu_\tau$, the hadronic mass spectra and branching ratio from this mode were also measured and the results used directly to improve our Monte Carlo modelling.

3.1. Analysis of $\tau^- \to K^0_S\pi^-\pi^0\nu_\tau$

To select events of the type $e^+e^- \to \tau^+\tau^-$ with one tau-lepton decaying to $K^0_S\pi^-\pi^0\nu_\tau$, the event is first divided into two hemispheres in the center-of-momentum system (CMS) using the thrust axis. One hemisphere of the event is required to contain only one charged track; this is defined as the tag hemisphere. The other hemisphere is required to have three charged tracks; this is called the signal hemisphere. The tag track and at least one of the signal hemisphere tracks are required to originate from the interaction point.

Approximately 35% of τ-leptons decay to fully leptonic final states. Requiring the track in the tag hemisphere to be identified as an electron or muon while requiring the signal hemisphere to contain only hadrons strongly reduces backgrounds from $e^+e^- \to q\overline{q}$ events. Electrons are identified using specialized likelihood selectors, whereas a neural network is used to identify muon tracks.

K^0_S candidates are constructed from any two oppositely charged tracks with an invariant mass within 25 MeV/c^2 of the K^0_S mass, 497.672 MeV/c^2 [9]. Only events with exactly one K^0_S candidate are retained. The track from the signal side not originating from the K^0_S candidate is required to be identified as a pion and originate from the interaction point. Pions are identified by dE/dx in the tracking system, the shape of the shower in the calorimeter and information from the DIRC. All tracks on the signal side are required to lie within the geometrical acceptance region of the EMC and DIRC to ensure good particle identification.

In addition, the net charge of the event must be zero and the thrust of the event is required to be greater than 0.85 to reduce the non-τ background.

Backgrounds from Bhabha events are suppressed by requiring the momentum of the tag-side track to be less than 4.9 GeV/c. Backgrounds from radiative Bhabha and μ-pair events with a converted photon are suppressed by requiring the modulus of the cosine of the decay angle to be less than 0.97. The decay angle is defined as the angle between the momentum of the π^+ originating from the K^0_S in the K^0_S's rest frame and the K^0_S momentum vector in the laboratory frame. When this quantity is calculated for e^+e^- conversion pairs misidentified as pions, its value is concentrated near ±1. From studies of missing transverse event energy, backgrounds from two-photon events are determined to be negligible. We also require exactly one identified π^0 in the event; the trajectory of the π^0 must be within 90 degrees of the $K^0_S\pi^-$ momentum vector. This ensures that the π^0 is more likely to be from the same τ as the $K_S\pi$. The neutral energy not attributed to the K^0_S or the π^0 must be less then 100 MeV. This should be very small anyway, but the cut is to reject unwanted photons. The energy of the π^0 in the center-of-mass system must be greater than 1.2 GeV. This cut is to remove the large background contribution in the region below 1.2 GeV. Figure. 2 shows the distribution of the π^0 energy.
The branching fraction $\mathcal{B}(\tau^- \to \bar{K^0}\pi^-\pi^0\nu_\tau)$ is estimated by

$$\mathcal{B}(\tau^- \to \bar{K^0}\pi^-\pi^0\nu_\tau) = \frac{1}{2N_{\tau\tau}} \frac{N_{\rm data} - N_{\rm bkg}}{\varepsilon'_{\rm sig}}, \qquad (4)$$

where $N_{\tau\tau}$ is the total number of $\tau^+\tau^-$ pairs in the data, $N_{\rm data}$ is the number of selected events in data, $N_{\rm bkg}$ is the number of background events estimated from Monte Carlo, and $\varepsilon'_{\rm sig}$ is the corrected signal efficiency to include K^0_S and K^0_L mesons.

The hadronic mass distributions for the different combinations of final state hadrons are also extracted, and used to tune our Monte Carlo. Figure 3 below shows the mass distribution for $K^0_S\pi^-$ from $\tau^- \to K^0_S\pi^-\pi^0\nu_\tau$, overlayed with the new Monte Carlo generated using this analysis.

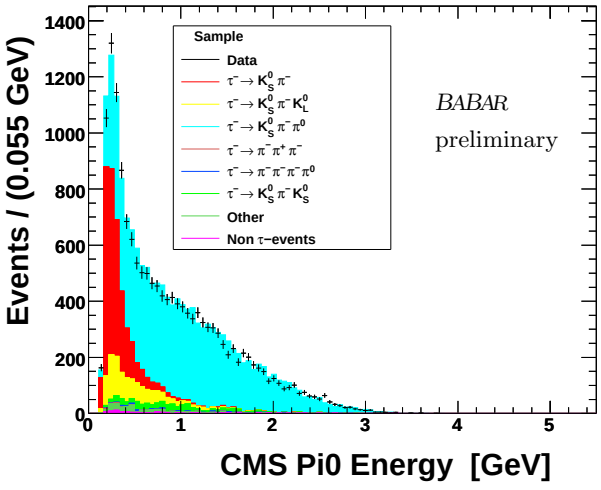

Figure 2: Distribution of the π^0 energy.

Table I $\mathcal{B}(\tau^- \to \bar{K}^0\pi^-\pi^0\nu_\tau)$ measured in this analysis.

Sample	$\mathcal{B}(\tau^- \to \bar{K}^0\pi^-\pi^0\nu_\tau)$ [%]
e-tag	$0.353 \pm 0.008\,(\text{stat}) \pm 0.016\,(\text{syst})$
μ-tag	$0.329 \pm 0.008\,(\text{stat}) \pm 0.016\,(\text{syst})$
Combined	$0.342 \pm 0.006\,(\text{stat}) \pm 0.015\,(\text{syst})$

3.2. Fit to $\tau^- \to K^0_S\pi^-\nu_\tau$ mass spectrum

The analysis of the decay $\tau^- \to K^0_S\pi^-\nu_\tau$ is a fit of the hadronic mass distribution to a parametric function describing the resonant structure. From this we obtain precise values for the mass and width of the

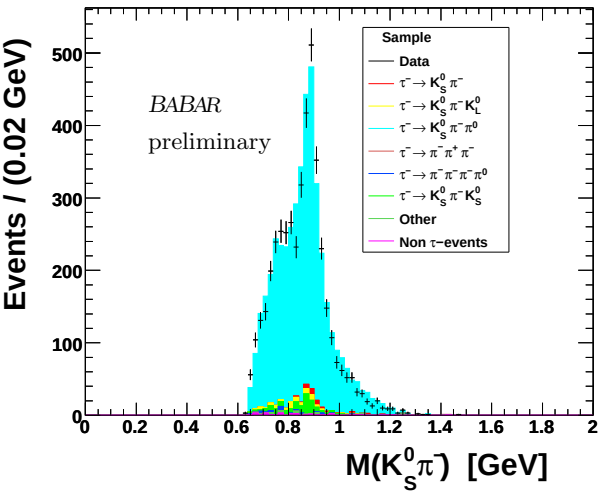

Figure 3: The data (points) and tuned Monte Carlo (blue) prediction for the $K^0_S\pi$ mass distribution from the $\tau^- \to K^0_S\pi^-\pi^0\nu_\tau$ signal mode.

K*(892) as well as information on other resonances present in the spectrum.

We denote the number of events found in bin i (without background subtraction) by n_i. The prediction for the expectation value of n_i, $\nu_i = E[n_i]$, can be written

$$\nu_i = \sum_{j=1}^{M} R_{ij}\mu_j + \beta_i \,, \tag{5}$$

where β_i is the expected number of background events, μ_j is the predicted number of signal events in bin j before detector effects (the "true" distribution), and R_{ij} is a response matrix that reflects the limited efficiency and resolution of the detector. The value of R_{ij} is

$$R_{ij} = P(\text{found in bin } i \,|\text{true value in bin } \ j) \,, \tag{6}$$

and thus the efficiency for bin j is found by summing over all bins where the event could be found. The predicted number of events in bin j of the true distribution can be written

$$\mu_j = \mu_{\text{tot}} \int_{\text{bin}\,j} f(m;\vec{\theta})\, dm \,, \tag{7}$$

where m denotes the $K^0_S\pi^-$ invariant mass and $\vec{\theta}$ represents a set of parameters.

The probability density function (pdf) $f(m;\vec{\theta})$ can be written [8]:

$$f(m;\vec{\theta}) \;\propto\; \frac{1}{s}\left(1-\frac{s}{{m_\tau}^2}\right)\left(1+2\frac{s}{{m_\tau}^2}\right) \times\; P\left(P^2|F_V|^2 + \frac{3({m_K}^2-{m_\pi}^2)^2}{4s(1+2\frac{s}{{m_\tau}^2})}|F_S|^2\right)$$

where $s = m^2$. Here the vector form factor F_V is given by

$$F_V = \frac{1}{1+\beta+\gamma}[BW_{K^1}(s)+\beta BW_{K^2}(s)+\gamma BW_{K^3}(s)] \,.$$

This form allows for the K*(892) and two additional vector resonances. The quantities β and γ are complex interference terms between the resonances, and the BW terms refer to the to relativistic Breit-Wigner functions for the specific resonance, given by

$$BW_R(s) = \frac{M_R^2}{s - M_R^2 + i\sqrt{s}\Gamma_R(s)} \,. \tag{8}$$

The energy dependent width is given by

$$\Gamma_R(s) = \Gamma_0 R \frac{M_R^2}{s}\left(\frac{P(s)}{P(M_R^2)}\right)^{2\ell+1} \,, \tag{9}$$

where

$$P(s) = \frac{1}{2\sqrt{s}}\sqrt{(s-M_+^2)(s-M_-^2)} \,, \tag{10}$$

and where $M_- = M_K - M_\pi$, $M_+ = M_K + M_\pi$, and ℓ is orbital angular momentum. Thus one has $\ell = 1$ if the $K\pi$ system is from a P-wave (vector), or $\ell = 0$ if the $K\pi$ system is from an S-wave (scalar).

The scalar form factor requires a different parametric function and can include contributions from the $K_0^*(800)$ and $K_0^*(1430)$ signals. This is

$$F_S = \varkappa \frac{s}{M^2_{K_0^*(800)}} BW_{K_0^*(800)}(s) + \lambda \frac{s}{M^2_{K_0^*(1430)}} BW_{K_0^*(1430)}(s)\,. \quad (11)$$

Each of the background modes is subtracted from the data, and then a least-squares fit is performed to the resulting mass spectrum. The fit model includes τ_j as a scale factor that relates the luminosity of the Monte Carlo sample for mode j to that of the data, and r_j as a factor that allows for the uncertainty in the prediction of the rate of the background process. The best estimate of r_j is equal to unity, but this is treated as a Gaussian distributed quantity with a standard deviation equal to the relative uncertainty on the production rate for the jth background mode.

The uncertainties in the values of other nominally fixed model parameters, e.g., the resonance parameters of the K*(1410), can be incorporated into the fit in a similar way. For a given parameter η one has a previously estimated value $\hat{\eta}$ and standard deviation σ_η, taken from the PDG. One includes in the minimisation function a Gaussian term in η centered about $\hat{\eta}$ with a standard deviation σ_η, and regards η as an adjustable parameter.

We also include terms in the minimisation which account for the uncertainty in the shapes of background mass distributions. This is particularly true for the $K^0_S\pi^- K^0_L$ mode, as it makes a larger contribution and the information on its shape is based largely on lower-statistics measurements from LEP [10]. We introduce two additional adjustable parameters, $\vec{\alpha} = (\alpha_1, \alpha_2)$, which have the effect of shifting and stretching the shape of the distribution [11]. This transformation is applied to the m_{ij} values for the $K^0_S\pi^- K^0_L$ background mode and the altered values are then used in the minimisation. The fitting procedures described above have been carried out using a variety of hypotheses. Figure 4(a) shows that a single K*(892) is clearly not enough to model the mass spectrum accurately. This was seen by the Belle collaboration [8], which proposed that the distribution should contain contributions from a $K_0^*(800)$ scalar and K*(1410) vector resonances.

In the region around 1.4 GeV in Fig. 4(a), the data are significantly higher than the fitted curve.The addition of the K*(1410) gives a significant improvement to the high mass region, yielding a χ^2 of 130.04 for 95 degrees of freedom. In these fits the rate of the K*(1410) was allowed to vary within the error given in the PDG.

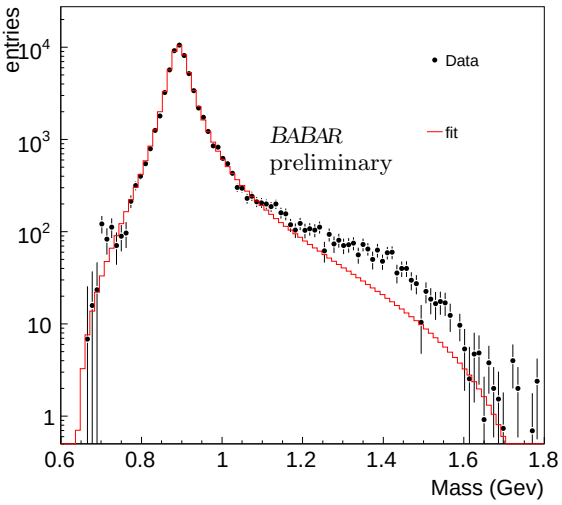

(a)

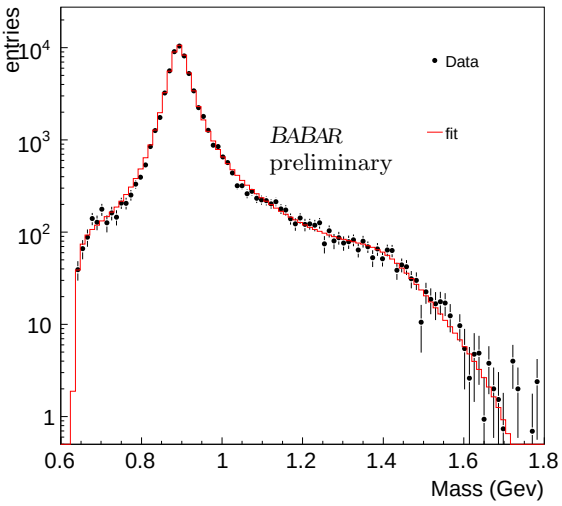

(b)

Figure 4: A fit to the $\tau^- \to K^0_S\pi^-\nu_\tau$ mass distribution using (a) single K*(892) resonance, (b) a combination of $K_0^*(800)$ + K*(892) + K*(1410).

The inclusion of the $K_0^*(800)$ further reduces our χ^2 to 113.05 for 94 degrees of freedom. This is a significantly better goodness-of-fit value than our K*(892) + K*(1410) fit model. For the mass and width of the $K_0^*(800)$ we use the measurements from the BES collaboration [12], $M = 841 \pm 30^{+81}_{-73}$, $\Gamma = 618 \pm 90^{+96}_{-144}$. The result is shown in Fig. 4(b).

If instead of a K*(1410) one uses a scalar $K_0^*(1430)$, one finds a comparable χ^2 value of 114.11 for 94 de-

grees of freedom. As such the K*(1410) and $K_0^*(1430)$ cannot be differentiated on their χ^2 value. To study what combination of K*(1410) and $K_0^*(1430)$ are present, one could exploit the different spins of the two resonances by carrying out an angular analysis. This is not part of the current study. The resulting values for the mass and width of the K*(892) are found to be

$$\begin{aligned} M(K^*(892)^-) &= 894.57 \pm 0.19\,(\text{stat.})\,\text{MeV/c}^2 \\ \Gamma(K^*(892)^-) &= 45.89 \pm 0.43\,(\text{stat.})\ \text{MeV/c} \end{aligned}$$

The statistical errors quoted already cover a number of systematic uncertainties such as those in the rates and shapes of backgrounds, which were incorporated by including corresponding adjustable parameters in the fit. Several additional sources of systematic uncertainty are also taken into consideration. The response matrix R_{ij} is derived from the Monte Carlo simulation of the detector. As a conservative estimate of the uncertainty of the detector response, which is dominated by modelling of the tracking and Calorimeter, we have varied the parameters of the response matrix by up to $\pm 10\%$. As a check of the fitting method we have taken a fully reconstructed Monte Carlo sample of signal events, and fitted them using the signal model. As the MC generator models the $\tau^- \to K_S^0\pi^-\nu_\tau$ decay with only the K*(892) resonance, the fit model also only contained this resonance. A further uncertainty in the fit model stems from the choice of resonances.We take the difference in the mass and width values for the K*(892) between our nominal fit and the alternative models which also yield comparable χ^2 values, as an estimate of the systematic uncertainty. The quadratic sum of all these sources of systematic uncertainty lead to an error on M(K*(892)) and Γ(K*(892)) of 0.19 MeV/c^2 and 0.57 MeV/c respectively.

4. Summary and Conclusion

Measurements of the τ mass and $\tau^+ - \tau^-$ mass difference have been carried out yielding results of:

$$M_\tau = 1776.68 \pm 0.12(\text{stat.}) \pm 0.41(\text{syst.})\,\text{MeV}/c^2.$$

$$\frac{M_{\tau^-} - M_{\tau^+}}{\langle M \rangle} = -3.4 \pm 1.3(\text{stat.}) \pm 0.3(\text{syst.}) \times 10^{-4}.$$

where $\langle M \rangle$ is the average of M_{τ^+} and M_{τ^-}. The τ mass result is in good agreement with the world average. We also find the mass difference result to be consistent with the results published by the Belle Collaboration at 1.8σ.

We have also carried out studies of the decays $\tau^- \to K_S^0\pi^-\nu_\tau$ and $\tau^- \to K_S^0\pi^-\pi^0\nu_\tau$ using 384.6 fb^{-1} of data. We have measured the branching ratio for $\tau^- \to \bar{K^0}\pi^-\pi^0\nu_\tau$, which is found to be:

$$\begin{aligned} &\mathcal{B}(\tau^- \to \bar{K^0}\pi^-\pi^0\nu_\tau) = \\ &(0.342 \pm 0.006\,(\text{stat.}) \pm 0.015\,(\text{sys.}))\% \,. \end{aligned}$$

For the $\tau^- \to K_S^0\pi^-\pi^0\nu_\tau$ mode we have measured the mass distributions of different combinations of final state hadrons: $\pi^-\pi^0$, $K_S^0\pi^-$, $K_S^0\pi^0$ and $K_S^0\pi^-\pi^0$. These were used to make important improvements to the `TAUOLA` Monte Carlo generator, which allowed for a precise estimation of the background contribution from this mode in the analysis of the $\tau^- \to K_S^0\pi^-\nu_\tau$ channel.

We have carried out a fit of the hadronic mass distribution for $\tau^- \to K_S^0\pi^-\nu_\tau$. This yields precise measurements for the mass and width of the K*(892) resonance:

$$\begin{aligned} &M(K^*(892)^-) = \\ &894.30 \pm 0.19\,(\text{stat.}) \pm 0.19\,(\text{syst.})\,\text{MeV/c}^2 \,, \end{aligned}$$

$$\begin{aligned} &\Gamma(K^*(892)^-) = \\ &45.56 \pm 0.43\,(\text{stat.}) \pm 0.57\,(\text{syst.})\,\text{MeV/c} \,. \end{aligned}$$

These values confirm the Belle collaboration's measurements [8] that indicated a K*(892) mass several MeV higher and a width several MeV lower than the world average. The results reported here represent a factor of two improvement in precision relative to the Belle measurements. We analyse the possibility of other resonances being present in this mass spectrum, and conclude that a combination of K*(800), K*(892) and K*(1410) provides a good description of the data. Figure 5 shows the results of various measurements that went into calculating the 2008 PDG average values for the mass and width of the K*(892). The Belle 2007 result and our result both indicate a shift towards 895 MeV for the mass value.

Acknowledgments

We are grateful for the extraordinary contributions of our PEP-II colleagues in achieving the excellent luminosity and machine conditions that have made this work possible. The success of this project also relies critically on the expertise and dedication of the computing organizations that support *BABAR*. The collaborating institutions wish to thank SLAC for its support and the kind hospitality extended to them. This work is supported by the US Department of Energy and National Science Foundation, the Natural Sciences and Engineering Research Council (Canada), the Commissariat à l'Energie Atomique and Institut National de Physique Nucléaire et de Physique des Particules (France), the Bundesministerium für Bildung und Forschung and Deutsche Forschungsgemeinschaft (Germany), the Istituto Nazionale di Fisica Nu-

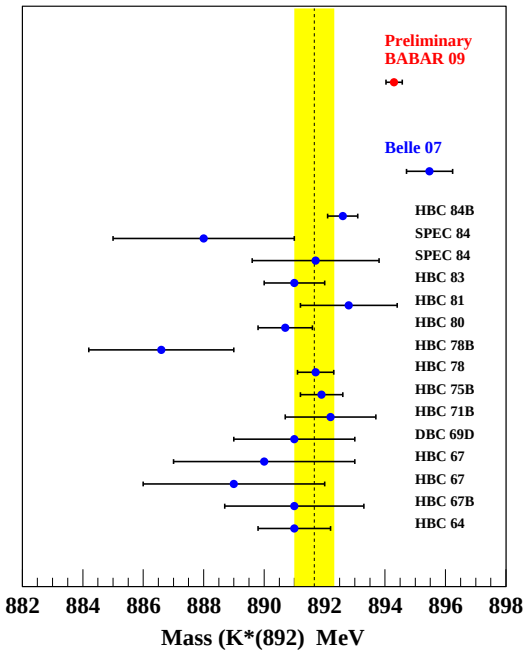

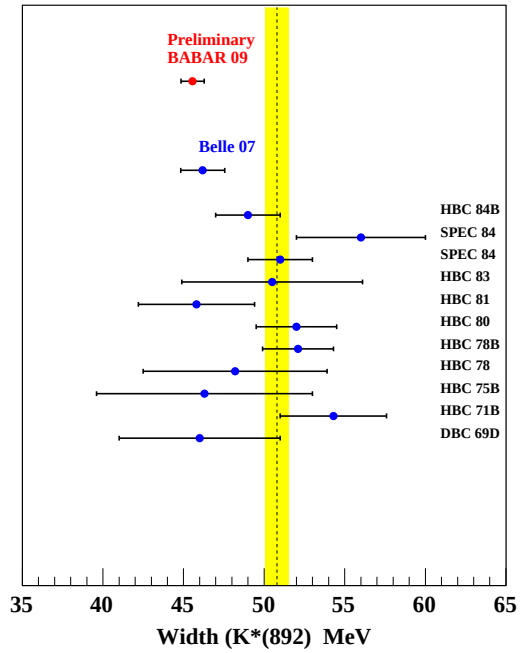

Figure 5: Comparison of the K*(892) mass and width values which were included in the PDG [3] calculated average value and the recent result from Belle, and our result. The majority of the PDG values are from hydrogen bubble chamber experiments.

cleare (Italy), the Foundation for Fundamental Research on Matter (The Netherlands), the Research Council of Norway, the Ministry of Education and Science of the Russian Federation, Ministerio de Educación y Ciencia (Spain), and the Science and Technology Facilities Council (United Kingdom). Individuals have received support from the Marie-Curie IEF program (European Union) and the A. P. Sloan Foundation.

References

[1] B. Aubert *et al.*, Nucl. Instrum. Meth. **A479** (2002) 1.
[2] B. Aubert [The BaBar Collaboration], arXiv:0909.3562 [hep-ex].
[3] C.Amsler *et al*, (Particle Data Group) Physics Letters **B667**,1 (2008).
[4] The ARGUS Collaboration, H. Albrecht *et al*, Phys. Lett. B **292**, 221 (1992).
[5] The Belle Collaboration, K. Belous *et al*, Phys Rev. Lett.**99**, 011801 (2007).
[6] B. Aubert *et al.*, *Measurement of* $\mathcal{B}(\tau^- \to K^0_S\pi^-\nu_\tau)$ *using the BaBar detector*, arXiv:0808.1121 (hep-ex).
[7] S. Jadach, Z. Was, R. Decker and J.H. Kühn, Comput. Phys. Commun. **76** (1993) 361.
[8] D. Epifanov *et al.* [Belle Collaboration], Phys. Lett. B **654**, 65 (2007) [arXiv:0706.2231 [hep-ex]].
[9] W. M. Yao *et al.* [Particle Data Group], J. Phys. G **33**, 1 (2006).
[10] R.Barate *et al*, Eur.Phys.J.C4:29-45,1998.
[11] G. Cowan, *Increasing the flexibility of a distribution to allow for systematic uncertainty*, RHUL internal note, `www.pp.rhul.ac.uk/~cowan/stat/notes/AltHist.pdf` (2009).
[12] M. Ablikim *et al.* [BES Collaboration], Phys. Lett. B **633**, 681 (2006) [arXiv:hep-ex/0506055].